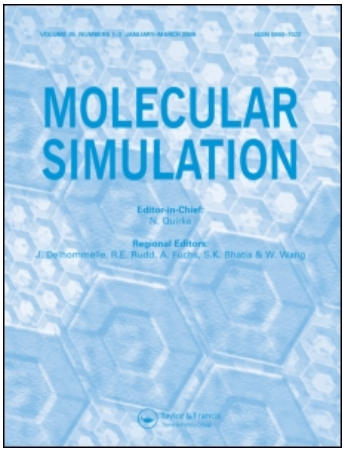

Molecular Simulation
Publication details, including instructions for authors and subscription information:
http://www.informaworld.com/smpp/title~content=t713644482

Molecular Dynamics Simulation of Platinum Particles Between Graphite Walls

Steven Y. Liem[a]; Kwong-Yu Chan[a]; Robert F. Savinell[b]
[a] Department of Chemistry, The University of Hong Kong, Hong Kong [b] Department of Chemical Engineering, Case Western Reserve University, Cleveland, Ohio, U.S.A.

To cite this Article Liem, Steven Y. , Chan, Kwong-Yu and Savinell, Robert F.(1994) 'Molecular Dynamics Simulation of Platinum Particles Between Graphite Walls', Molecular Simulation, 13: 1, 47 — 60
To link to this Article: DOI: 10.1080/08927029408022184
URL: http://dx.doi.org/10.1080/08927029408022184

Molecular Simulation, 1994, Vol. 13, pp. 47–60
Reprints available directly from the publisher
Photocopying permitted by license only

MOLECULAR DYNAMICS SIMULATION OF PLATINUM PARTICLES BETWEEN GRAPHITE WALLS

STEVEN Y. LIEM AND KWONG-YU CHAN*

Department of Chemistry, The University of Hong Kong, Pokfulam Road, Hong Kong

ROBERT F. SAVINELL

Department of Chemical Engineering, Case Western Reserve University, Cleveland, Ohio, 44106, U.S.A.

(Received July 1993, accepted November 1993)

We report preliminary molecular dynamics simulations results for platinum atoms confined between two parallel graphite surfaces. The system shows phase transition characteristics corresponding to a second order transition. Significant structural changes are also observed in the range of temperature studied. We have also investigated the effects of two dfferent Pt-wall interaction potentials: the 9-3 form suggested by Crowell and the 10-4 form originally proposed by Steele. The results show that the two systems have rather different structural characteristics but similar thermodynamic behaviour.

KEY WORDS: Molecular dynamics, platinum, carbon/graphite wall, adsorption

1 INTRODUCTION

The adsorption of fluids on solid substrates is of interest in many different fields. Adsorption is a key process in catalytic reactions, in separation processes, and other industrial activities. The properties of such systems have generated intense interest because of their potential applications in industry. In the past decade, a number of simulation studies have been reported for adsorbates on a substrate [1–6]. Most of these are for gas/solid systems like argon on solid CO_2 and liquid/solid systems like liquid nitrogen on graphite. Lennard-Jones liquids confined to micropores have also been studied extensively [7, 11] but relatively little work has been done on systems where metal particles are adsorbed on a solid substrate. These are of particular interest since they could be used as models of catalytic environment. In this respect, platinum (Pt) on carbon is an important catalyst with many applications, e.g. in electrochemical reactions. The aggregation dynamics and morphology of Pt particles near to a carbon surface under various conditions are of great interest [8, 9, 10]. These studies can be of assistance in optimising the performance of the Pt catalyst in catalytic reactions.

*Author to whom correspondence should be addressed.

This paper reports the results of a preliminary molecular dynamics (MD) simulation study of Lennard-Jones (LJ) type Pt confined between two smooth carbon surfaces. We have studied the behaviour of the Pt atoms and examined the thermodynamic and structural properties of the system under a wide range of temperatures. The effect of the Pt-wall interaction potential on the system is also examined by comparing two different Pt-wall interaction potentials.

2 DETAILS OF THE SIMULATIONS

In this study, a simple model of the Pt-carbon wall system is used in the simulations. The arrangement of the modelled system is similar to the one used by Walton and Quirke [11]. A diagrammatic representation of the system is shown in Figure 1. The two carbon walls are parallel to each other and are perpendicular to the z-axis. Normal periodic boundary conditions are maintained in the x and y directions.

We used only Pt-Pt and Pt-wall interactions to control the dynamics of the system. The Pt-Pt interaction is represented by the LJ 12-6 potential

$$\phi_{pp}(r) = 4\epsilon_{pp}\left\{\left(\frac{\sigma_{pp}}{r}\right)^{12} - \left(\frac{\sigma_{pp}}{r}\right)^{6}\right\} \tag{1}$$

where ϵ_{pp} and ϕ_{pp} are the well depth and the collision diameter for interactions, and r is the separation distance between the two Pt atoms. The behaviour of a noble gas near a Pt surface has been studied previously [12, 13, 14]. Unfortunately, in most of these articles the Pt is modelled as a substrate but not as a free atom. Garofalini and co-workers [15, 16, 17] have developed a set of LJ Pt-Pt potential parameters for their simulation works in the last few years. With this set of parameters, they obtained MD results of Pt on silicate that give good agreement with EXAFS studies [16,18] as well as other structural and dynamic experimental results [17]. We therefore choose to use the parameters adopted by Garofalini *et al.* with the values of ϵ_{pp}/k_b (k_b is the Boltzmann constant) and σ_{pp} being 7910 K and 2.54 Å respectively. Since these parameters have not been tested against

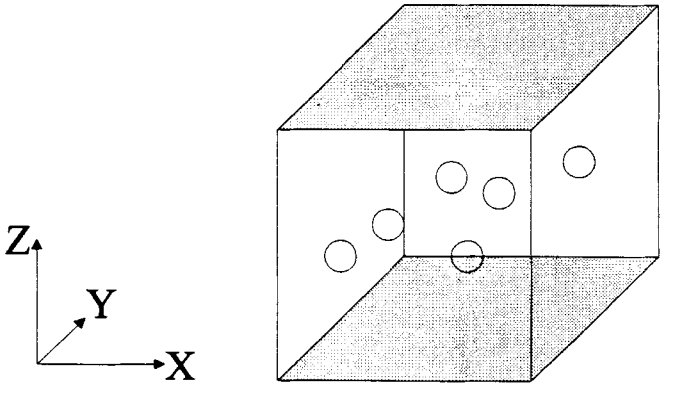

Figure 1 A diagrammatic representation of the simulated system.

the thermodynamic properties of Pt, e.g. phase equilibrium and critical proint, there exist some uncertainties as to the absolute values of energies obtained from Pt-carbon wall simulations. However, since good agreement with EXAFS studies exist for Pt on silicate simulation, we expect our simulations will yield at least qualitative results.

An integrated LJ potential is used for the interaction between a Pt particle and the graphite wall. For this kind of adsorbent/substrate interaction, various model potentials of the true interaction have been proposed in the past. Among these, the 9-3 and the 10-4 forms have been used extensively in simulation studies. The 9-3 form was first proposed by Crowell [19]. He suggested that the interaction potential between an adatom and the substrate can be approximated by performing integration of the potential over the entire substrate. The resultant potential has the 9-3 form

$$\phi_{pc}(z) = 2\pi\rho_c\epsilon_{pc}\left\{\left(\frac{\sigma_{pc}}{z}\right)^9 - \left(\frac{\sigma_{pc}}{z}\right)^3\right\} \tag{2}$$

where z is the distance between the platinum and the carbon walls and ρ_c is the reduced number density of carbon in the graphite boundaries calculated using the Lennard-Jones diarmeter σ_{cc}. For the solid state of common LJ type fluids, a typical value of ρ_c is 0.9. The σ_{pc} and ϵ_{pc} are the potential parameters for Pt-wall interaction. This 9-3 potential has been used by Lane and Spurling [20, 21] in their simulation study of the effects of adsorption on interparticle forces.

The other widely used substrate/adsorbent interaction potential is the 10-4 potential proposed by Steele [3]. This 10-4 potential function has since been simplified in various ways. The original form includes a periodic spatial term which accounts for the distribution of atoms in the substrate surface. However, we choose to use a simplified form [22] in this study where this spatial term is not included in the potential function. Similar to the 9-3 potential, this simplified 10-4 potential is a function of the z-distance between the substrate and the adatom:

$$\phi_{pc}(z) = 4\pi\rho_n\sigma_{pc}^6\epsilon_{pc}\left\{\frac{\sigma_{pc}^6}{5z^{10}} - \tfrac{1}{2}\sum_{i=0}^{n}\frac{1}{(z + i\triangle z)^4}\right\} \tag{3}$$

where n is the number of carbon layers to be used in the summation, $\triangle z$ is the distance between successive carbon layers which has a value of 3.35Å [22] and ρ_n is the solid surface number density which has a value of 0.382 atoms/Å^2. This surface density is based on the interatomic distance (1.42 Å) of carbon atoms in graphite lattice whereas in equation (2), the packing of carbon is based on effective LJ diameter $\sigma_{cc} = 3.46$Å. As a result, the corresponding number density value is somewhat higher than that of the 9-3 potential ($\rho_c = 0.9$). The major difference between the two potentials is that the substrate-adatom interaction is calculated in a layer by layer manner for the 10-4 potential. For this study, a three term summation is used for the evaluation of Pt-wall interaction.

Both of these potential functions have been used extensively in molecular simulations [20, 21]. The 9-3 potential is less complicated but it has been shown that it may underestimate the strength of substrate-adatom interaction under certain circumstances [3, 23]. A comparison of the two potential functions is shown in Figure 2. Both potential functions do not include the atomic structure of the carbon wall which could play an important role in determining the Pt structures near the wall.

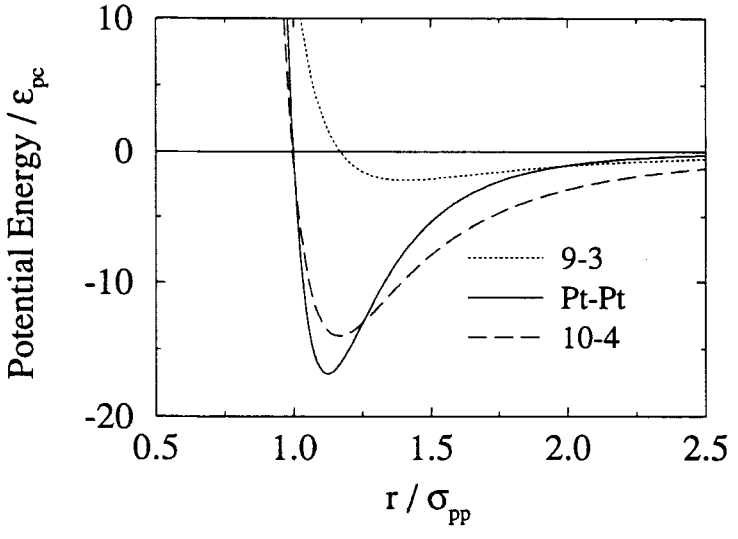

Figure 2 The Pt-Pt interaction potential and the Pt-wall interaction potentials. The dotted line is the 9–3 Pt-wall potential and the dashed line is the 10–4 Pt-wall potential. The solid line is the Pt-Pt interaction potential.

This preliminary study focuses on the effect of wall strength and the effect of wall structure will be investigated in the future. The effects of the dfference between the two Pt-wall potentials are investigated in this study and the consequences are discussed in section 3.3.

The potential parameters for the Pt-wall interaction can be obtained by using the Lorentz-Berthelot mixing rule

$$\epsilon_{pc} = (\epsilon_{cc}\,\epsilon_{pp})^{\frac{1}{2}}, \tag{4a}$$

$$\text{and} \qquad \sigma_{pc} = (\sigma_{pp} + \sigma_{cc})/2 \tag{4b}$$

The potential parameters for C-C interactions can be found in reference [3] and the values are $\epsilon_{cc}/k_B = 28$ K and $\sigma_{cc} = 3.40$ Å. The ϵ_{pc} and σ_{pc} for Pt-wall interactions are 470 K and 2.97 Å, respectively. These potential parameters are only used as a first approximation for the Pt-wall interaction as no previous studies of Pt-carbon wall system can be found in the literature.

We have carried out a series of molecular dynamics simulations using the two different Pt-wall interaction potentials. All simulations were performed with a system containing 512 Pt atoms. The initial configuration contains Pt atoms in an arbitrary regular lattice structure. Random velocities corresponding to the desired system temperature are assigned to each Pt atom. A potential cut off distance of 3.5 σ_{pp} was used in all simulations and the Verlet leap frog algorithm [24] was used to integrate the equations of motion. The reduced density ($\rho^* = N\sigma^3/V$) of the system is 0.0898 and the distance between the two carbon walls is chosen to be 10 σ_{pp}. The dimensions of the simulation box in X, Y and Z directions are 23.87, 23.87 and 10.00 σ_{pp} respectively.

The simulations were performed with the reduced temperature, $T^* = k_B\,T/\epsilon_{pp}$,

of the system ranging from 0.05 to 2.0. A time step size of 1.0 fs was used to integrate the equations of motion. The runs can be divided into two parts. In the first part, the system was equilibrated from the initial configuration to the specified state point. During this stage, the temperature of the system was controlled by using an *ad hoc* scheme [25]. This part normally requires about 100 ps of simulated time for high temperature systems and 500 ps for low temperature systems. The second part is the production run in which the temperature of the system is allowed to fluctuate spontaneously and the system evolves as in a micro-canonical ensemble. During this stage, both thermodynamic and structural properties of the system are accumulated. The results presented in this paper are averaged from run lengths of at least 100 ps.

3 RESULTS OF SIMULATIONS

3.1 *Results of simulations using the 9–3 potential*

For the 9–3 potential, simulations were carried out at 10 different state points each at a different temperature. Since no temperature control was imposed during the production run, the mean temperature of the system at the end of the run is slightly different from the desired temperature. However, the mean temperature of the system is still close to the specified temperature (within 5%). The results of the simulations are shown in table 1. The graph of potential energy against mean system temperature (Figure 3) shows that the slope changes significantly at $T^* \approx 0.4$ and $T^* \approx 1.0$. These are second order transitions and are believed to be the melting and boiling transitions, respectively.

The morphology of the Pt atoms also changes noticeably when the system is cooled from high temperature states. These can be seen from the reduced density profiles, $\rho^*(z)$, across the boundaries and the pair distribution functions, $g(r)$. The $\rho^*(z)$ is evaluated by dividing the space between the two boundaries into slabs of thickness Δz parallel to the walls. The number of Pt atoms in each slab, $n(z)$, is recorded during the course of a simulation. The final number in each slab is used to calculated the reduced density of that particular slab at the end of the run. The density profile, $\rho^*(z)$, between the two walls is given by

$$\rho^*(z) = \frac{n(z)\sigma_{pp}}{\Delta z L_x L_y N_{\text{sample}}} \tag{5}$$

Table 1 Results of simulations using the 9–3 potential functions.

*Averaged T**	*PE/(kJmol^{-1})*
0.049	-395
0.101	-401
0.204	-395
0.300	-399
0.410	-377
0.584	-309
0.819	-213
0.992	- 77
1.517	- 46
2.005	- 4

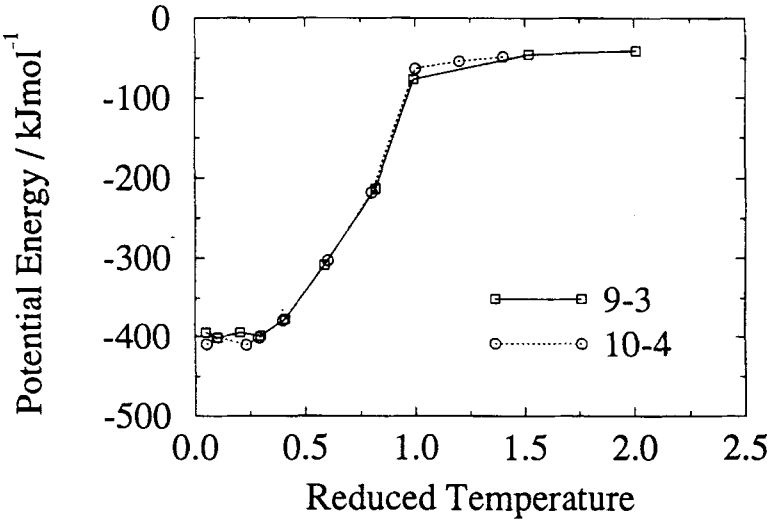

Figure 3 Potential energy against mean system temperature for the two simulations using different Pt-wall interaction potentials.

where L_x and L_y are the x- and y-dimension of the system and N_{sample} is the number of samples taken during the run. The $\rho^*(z)$ presented in this paper is calculated from 200 slabs.

The predicted $\rho^*(z)$ of the system at different temperatures are shown in Figure 4. At high temperatures, $\rho^*(z)$ has a maximum in the central region with no noticeable build up of Pt atoms adjacent to the walls. The Pt atoms tend to cluster together in the central region. For the low temperature states, density peaks start to appear in $\rho^*(z)$. This is most obvious for $T^* = 0.4$ indicating the development of ordering among the Pt atoms. However, the $\rho^*(z)$ for systems with $T^* < 0.2$ suggest that the Pt atoms are in an amorphous state where ordering of the Pt atoms can only be observed in part of the system. This is believed to be due to too high a cooling rate used in the simulations. As a result, the system is trapped in a metastable state. The peaks in $\rho^*(z)$ at different temperatures show that the arrangement of Pt atoms is gradually changing to become more layer like. No significant adsorption of Pt atoms onto the carbon walls can be observed even for the lowest temperature system. This could be due to the relatively weak Pt-wall interaction in comparison with the stronger Pt-Pt interaction.

We have also calculated the Pt-Pt pair distribution function using the conventional method [26] in order to obtain some qualitative information about the Pt atoms in the system. At high temperatures (e.g. $T^* = 1.0$), the $g(r)$ has only one broad peak at $r = 1$ and beyond that, it is smooth and decreases gradually (Figure 5a). At lower temperatures, the $g(r)$ generally has more than one prominent peak (Figure 5b) and the peaks become more well defined as the temperature decreases. These peaks were mostly found in the range of $r = 1.0$ to 3.5 σ_{pp} beyond which no well-defined peaks can be identified. These facts are consistent with the structural characteristics of the Pt atoms observed in $\rho^*(z)$. At high temperatures, both $g(r)$ and $\rho(z)$ indicate that there is no significant local ordering of Pt atoms. However,

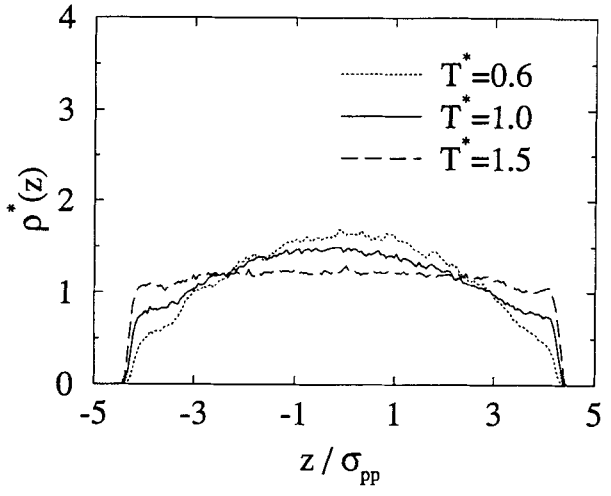

Figure 4a Relative density profiles of the 9–3 system at $T^* = 0.6$, 1.0 and 1.5.

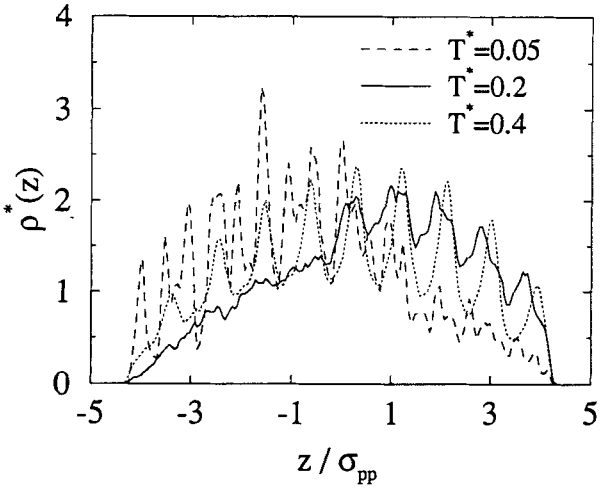

Figure 4b Relative density profiles of the 9–3 system at $T^* = 0.05$, 0.2 and 0.4.

short ranged order is developed and observed in both $g(r)$ and $\rho^*(z)$ at lower temperatures.

3.2 *Results of simulations using the 10–4 potential*

Similar simulations were carried out for the 10–4 potential at corresponding system temperatures. The range of temperature is between $T^* = 0.05$ to 1.4. The results in table 2 show that the variation of potential energy with temperature is similar to those of the 9–3 system. Two transitions can be identified in the graph of

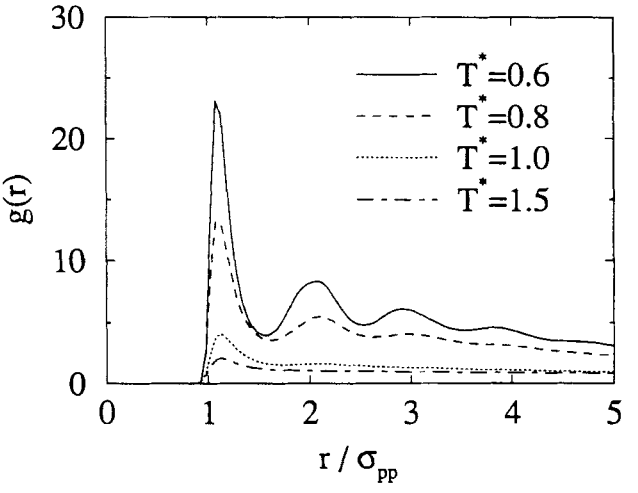

Figure 5a Pair distribution functions of the 9-3 system at $T^* = 0.6$, 0.8, 1.0 and 1.5.

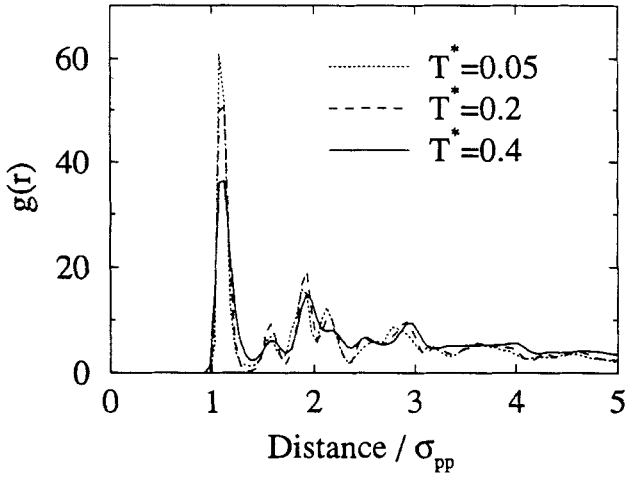

Figure 5b Pair distribution functions of the 9-3 system at $T^* = 0.05$, 0.2 and 0.4.

potential energy against temperature (Figure 3) and the transitions take place at similar temperatures as in the 9-3 system.

The density profiles of the 10-4 system (Figure 6) are found to be different from that of the 9-3 system. For systems with $T^* \geq 1$, $\rho^*(z)$ appears to be fairly smooth and flat in the region between the two boundaries. However, a single sharp peak is found next to each boundary wall. The distance between the peak and the boundary is about 1.0 σ_{pp}. These two peaks show that Pt atoms are being adsorbed onto the carbon walls. For systems with lower temperatures ($T^* < 1$), density peaks appear in the region between the walls and the peaks become more prominent at

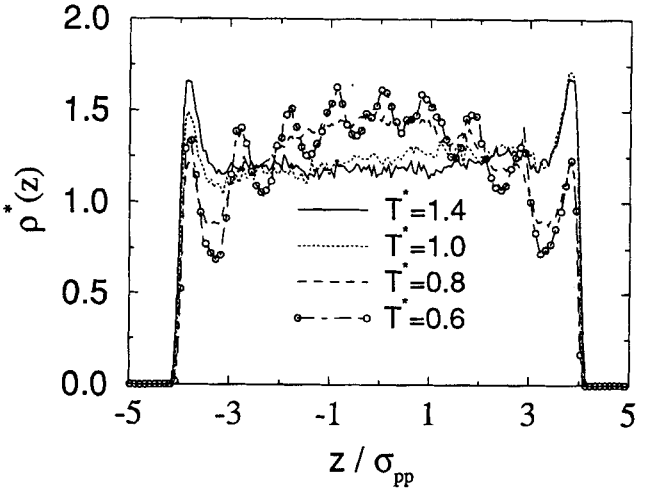

Figure 6a Relative density profiles of the 10–4 system at $T^* = 0.6$, 0.8, 1.0 and 1.4.

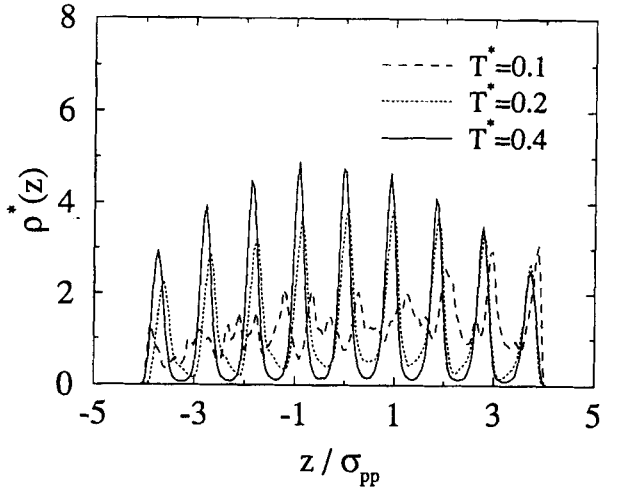

Figure 6b Relative density profiles of the 10–4 system at $T^* = 0.1$, 0.2 and 0.4.

lower temperatures. These peaks become so distinct for systems with $T^* < 0.5$ that the Pt atoms are believed to be arranged layer by layer. Indeed, the *XZ* and *YZ* projections of a typical snapshot of the system (Figure 7) show that the Pt atoms are arranged in such a manner. To some extent, the small gap between the walls may enhance the formation of such an ordered layer structure. However, as in the 9–3 system, the two lowest temperature states are thought to be amorphous so that ordering of Pt atoms occur only in part of the system.

Table 2 Results of simulation using the 10–4 potential functions.

*Averaged T**	*PE/(kJmol^{-1})*
0.051	-410
0.102	-401
0.203	-410
0.288	-401
0.399	-380
0.600	-303
0.800	-218
1.000	- 63
1.200	- 54
1.400	- 48

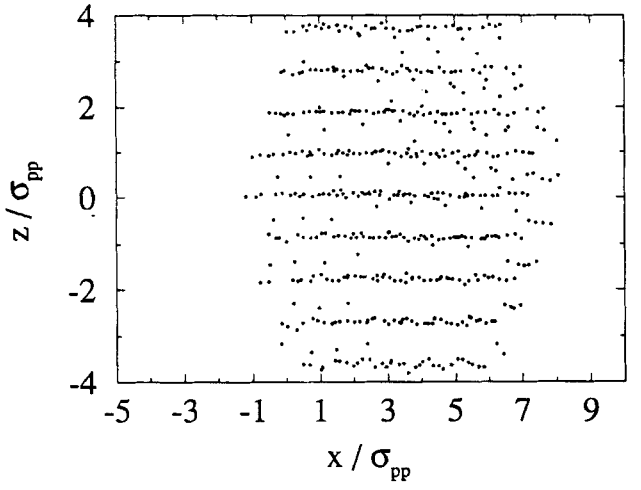

Figure 7a A typical snap shot of the 10–4 system at $T^* = 0.2$ (looking through the XZ plane).

The pair distribution functions, $g(r)$ have similar characteristics (Figure 8) to the 9–3 system. No long range order can be identified at high temperature. This can be shown by the fact that $g(r)$ has only one broad peak at a distance of about 1 σ_{pp} and beyond which it is flat. The number of peaks increases as the temperature of the system is decreased and the peaks become more distinct. For the $T^* = 0.2$ system, a distinct peak can be identified even at a distance of 4σ. This indicates that well defined local structure was formed among the Pt atoms at low temperature.

3.3 *Comparisons of the Pt-wall potentials*

The results illustrate that structural characteristics of the Pt atoms between the walls are quite different for different Pt-wall potentials. Firstly, there are noticeable difference in the tendency of Pt atoms to be adsorbed onto the carbon walls. The morphology of Pt atoms between the walls are also different. In the 9–3 system, the Pt atoms tend to form a cluster between the walls with no detectable adsorption

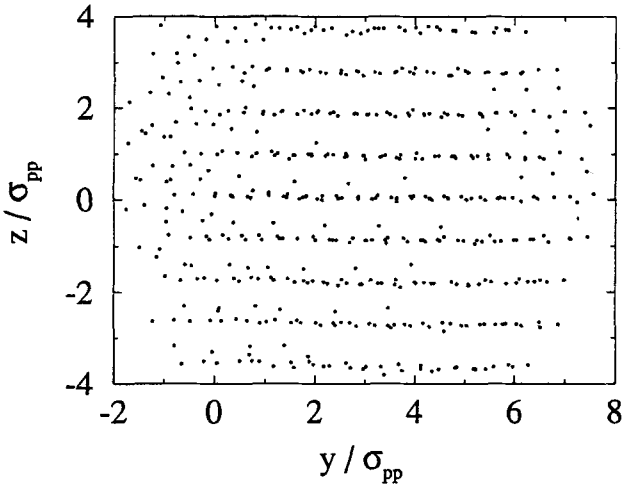

Figure 7b A typical snap shot of the 10–4 system at $T^* = 0.2$ (looking through the YZ plane).

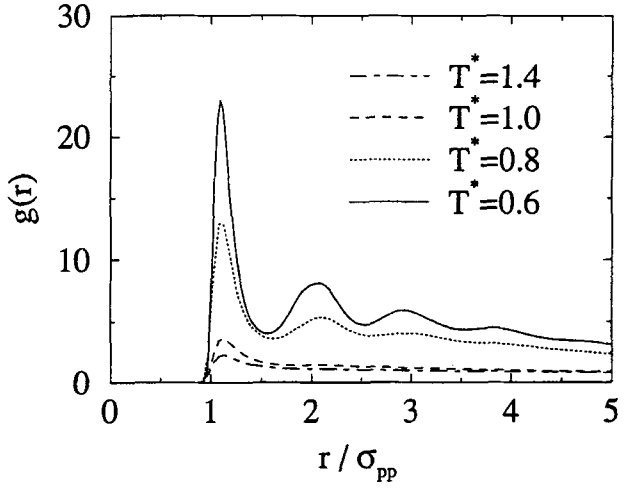

Figure 8a Pair distribution functions of the 10–4 system at $T^* = 0.6$, 0.8, 1.0 and 1.4.

of Pt atoms. In the 10–4 system, Pt atoms are distributed more evenly between the walls and Pt atoms are adsorbed onto the carbon walls. Nevertheless, the Pt atoms are arranged in an orderly state when the temperature of the system is sufficiently low for both Pt-wall potentials. This kind of ordering effect is quite common in confined systems. It has been observed previously in capillary systems [11] and non-equilibrium systems with both smooth [27] as well as structured boundaries [28, 29, 30, 31].

These structural differences may be inherent in the Pt-Wall potential function.

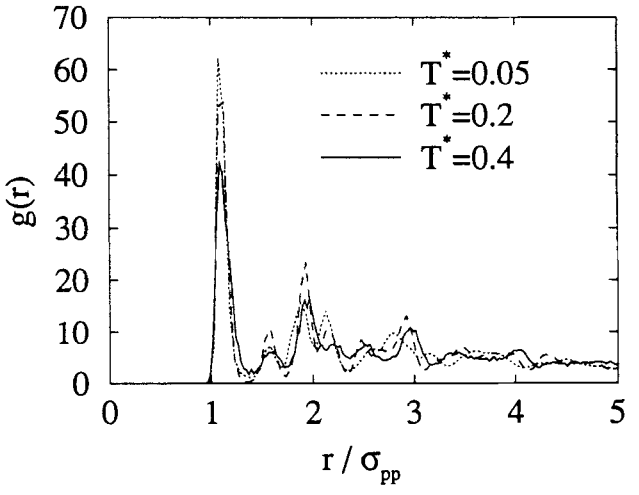

Figure 8b Pair distribution functions of the 10–4 system at $T^* = 0.05$, 0.2 and 0.4.

A comparison of the Pt-wall and the Pt-Pt interaction potential functions is shown in Figure 2. It shows that the 9–3 potential has a softer repulsive core relative to the 10–4 and the Pt-Pt interaction potentials. The potential minimum of the 9–3 function is closer to the carbon wall than the 10–4 potential. Perhaps more important is the fact that the 9–3 function has a shallower potential well in comparison with the other two potentials. This distinction between the 9–3 and the 10–4 potential is largely due to the difference in the constant factors appeared in their corresponding expressions. As a result, the structural differences are believed to be a direct result of the relative strengths of the Pt-wall and Pt-Pt interaction.

In spite of the structural dfferences, it is interesting to note that thermodynamically the two systems are fairly similar. This is illustrated by the fact that the transition temperatures of the two systems are almost identical. Intuitively, one would expect two systems with significant structural differences might exhibit dissimilar thermodynamic properties. This is an unexpected result which should be investigated in more detail.

4 CONCLUSIONS

The results of this study show that the use of different forms of the Pt-Wall potential have a significant effect on the structural characteristics of the system but thermodynamically, the effect is insignificant. As a result of the relatively weak Pt-wall interaction in the 9–3 system, no detectable adsorption of Pt atoms can be observed for the temperature range studied. On the other hand, Pt atoms are adsorbed by the carbon wall in the 10–4 system even at high temperatures.

The morphology of the Pt atoms changes significantly when both systems are cooled from high to low temperature states. At higher temperatures, Pt atoms are found to cluster in the region between the walls for the 9–3 system. For the 10–4

system, the Pt atoms are distributed more evenly between the walls. At low temperatures, Pt atoms in both systems tend to form a layered structure with well defined local structures. The 10–4 system is more successful in achieving such an orderly state. For all the systems studied, no isolated clusters or islands are observed which might be due to the insufficient size of the simulation cell and the chosen densities.

This is only a preliminary study of the Pt-carbon system. We are currently trying to optimize the potential parameters. Further simulations are also being carried out to study the morphology of the Pt atoms under different gap widths, system densities and molecularity of the graphite walls.

Acknowledgements

This work has been funded by the Hong Kong Research Grant Council (Award HKU 20/91). Some of the simulations were carried out on the San Diego Supercomputer Center (SDSC) through a grant available from Hong Kong City Polytechnic.

References

[1] J.T. Talbot, D.J. Tildesley, and W.A. Steele, "Molecular dynamics simulation of fluid N_2 adsorbed on a graphite surface", *Faraday Discuss. Chem. Soc.*, **80**, 91, (1985).
[2] Y.P. Joshi and D.J. Tildesley, "A simulation study of the melting of patches of nitrogen adsorbed on graphite", *Molecular Physics*, **5**, 999, (1985).
[3] W.A. Steele, "The physical interaction of gases with crystalline solids", *Surface Science*, **36**, 317, (1973).
[4] Y.P. Joshi and D.J. Tildesley, "Molecular dynamics simulation and energy minimization of O_2 adsorbed on a graphite surface", *Surface Science*, **166**, 169, (1986).
[5] K. Flurchick and R.D. Etters, "Epitaxial orientations of O_2 monolayers on graphite by superlattice formation", *J. Chem. Phys.*, **84**, 4657, (1986).
[6] V.R. Bhethanabotla and W.A. Steele, "Computer-simulation study of melting in dense oxygen layers on graphite", *Phy. Rev. B*, **41**, 9480, (1990).
[7] G.S. Heffelfinger, Z. Tan, K.E. Gubbins, U.M.B. Marconi and F. van Swol, "Lennard-Jones mixtures in a cylindrical pore. A comparison of simulation and density functional theory", *Molecular Simulation*, **2**, 393, (1989).
[8] L.J. Bregoli, "The influence of platinum crystallite Size on the electrochemical reduction of oxygen in phosphoric acid", *Electrochemica Acta*, **23**, 489, (1978).
[9] M. Watanabe, H. Sei and P. Stonehart, "The influence of platinum crystallite size on the electroreduction of oxygen", *J. Electrochem. Soc.*, **261**, 375, (1989).
[10] G.C. Bond, "The origin of particle size effects in Heterogeneous catalysts", *Surface Science*, **56**, 966, (1985).
[11] J.P.R.B Walton and N. Quirke, "Capillary condensation: A molecular simulation study", *Molecular Simulation*, **2**, 361, (1989).
[12] J.E. Black and P. Bopp, "Orientation of small rafts of xenon atoms physisorbed on Pt(111)", *J. Chem. Phys.*, **34**, 7410, (1986).
[13] J.E. Black and A-Janzen, "Uniaxial strain events in molecular-dynanmics simulations of small rafts of xenon physisorbed on Pt(111)", *J. Chem. Phys.* **38**, 8494, (1988).
[14] A.P.J. Jansen, "Molecular dynamics study of the coverage dependence of Xe desorption from Pt(111)", *J. Chem. Phys.*, **97**, 5205, (1992).
[15] S.M. Levine and S.H. Garofalini, "Interactions of Pt single atoms with the vitreous silica surface; Adsorption and thermal accommodation", *Surface Science*, **177**, 157 (1986).
[16] S.M. Levine and S.H. Garofalini, "Computer simulation of interactions of model Pt particles and films with the silica surface", *J. Chem. Phys.*, **88**, 1242, (1988).
[17] D.C. Athanasopoulos and S.H. Garofalini, "Molecular dynamics simulations of the effect of adsorption of SiO_2 surfaces", *J. Chem Phys.*, **97**, 3775, (1992).
[18] S.M. Levine and S.H. Garofalini, "Molecular dynamics simulation of Pt on a vitreous silica surface", *J. Chem. Phys.*, **163**, 59, (1985).

[19] A.D. Crowell, "Potential energy functions for graphite", *J. Chem. Phy.*, **29**, 446, (1958).
[20] J.E. Lane and T.H. Spurling, "Monte-Carlo simulations of the effects of adsorption of interparticle forces", *Aust. J. Chem.*, **33**, 231, (1980).
[21] J.E. Lane and T.H. Spurling, "The thermodynamics of a new type of surface transition", *Aust. J. Chem.*, **34**, 1529, (1981).
[22] L.L. Lee, "Molecular Themodynamics of Nonideal Fluids", Butterworths, Boston, 1988, pp. 423–429.
[23] J.M.D. Macelroy and H.-H. Suh, "Simulation studies of a Lennard-Jones Equid in micropores", *Molecular Simulation*, **2**, 313, (1989).
[24] L. Verlet, "Computer 'experiments' on classical fluids. I. Thermodynamical properties of Lennard-Jones molecules", *Phys. Rev.*, **159**, 98, (1967).
[25] W.T. Ashurst and W.G. Hoover, "Dense fluid shear viscosity via non-equilibrium molecular dynamics", *Rhys. Rev. A*, **11**, 658, (1975).
[26] D.J. Tildesley and M.P. Allen, "Computer simulation of liquids", 2nd Ed., Clarendon Press, Oxford, 1989, pp. 182–185.
[27] G. Ciccotti and C. Trozzi, "Stationary non-equilibrium states by molecular dynamics. II. Newton's law", *Phys. Rev. A*, **29**, 916, (1984).
[28] S. Sharma and L.V. Woodcock, "Interfacial viscosities via stress auto-correlation functions", *J. Chem. Soc. Faraday Trans.*, **87**, 2023, (1991).
[29] P.A. Thompson and M.O. Robbins, "Shear flow near solids: epitaxial order and flow boundary conditions", *Phy. Rev. A*, **41**, 6830, (1990).
[30] J. Koplik, J.R. Bannavar and J.F. Willemsen, "Molecular dynamics of fluid flow at solid surfaces", *Physics of Fluid A, Fluid Dyn.*, **1**, 781, (1989).
[31] S.Y. Liem, D. Brown and J.H.R. Clarke, "A comparison of the homogenous shear & sliding boundary methods of determining fluid viscosities using NENM", *Phys. Rev. A*, **45**, 3706, (1992).